doi.org/10.36721/PJPS.2025.38.5.REG.14310.1

Isolation and characterization of a novel chalcone derivative from *Arisaema utile* a selective MAO-B inhibitor in sodium azide-induced rat model

Muhammad Kamran Khan and Malik Saadullah*
Department of Pharmaceutical Chemistry, GC University Faisalabad, Pakistan

Abstract: This study aims to investigate the neuroprotective effects of Utilito, a novel chalcone derivative isolated from *Arisaema utile* in a sodium azide-induced Alzheimer's disease (AD) rat model. Anti-alzheimer activities were assessed through *in silico* molecular docking, simulation studies and in *vivo* studies. Utilito at doses of 100, 200, 300 mg/kg was administered in Wistar rats (n=6/group) for 14 days. Cognitive performance and locomotion were assessed through behavioural tests (Morris water maze, Y-maze, and open field). Biochemical assays measured the levels of oxidative stress biomarker including catalase (CAT) superoxide dismutase (SOD), reduced glutathione (GSH), and malondialdehyde (MDA). Molecular docking studies revealed a strong binding affinity of Utilito with monoamine oxidase (MAO-B), with a docking score of -41.4 kJ/mol. Conventional hydrogen bond interactions were observed between the MAO-B residues LEU171, TYR398, and TYR435 and the phenol ring of Utilito. Utilito also showed 71 ± 0.11% anti-oxidant activity in the DPPH assay. Behavioural tests utilizing animal models demonstrate the cognitive-enhancing effects of Utilito. Biochemical evaluations underscore the antioxidant properties of Utilito, offering valuable insights into their mechanisms of action at the cellular level. Utilito exhibits antioxidant activity and cognitive improvement in a rat AD model, suggesting its promise as a therapeutic candidate for AD.

Keywords: Chalcones, Alzheimer's disease, MAO-B inhibitor, molecular docking

Submitted on 17-03-2025 – Revised on 27-05-2025– Accepted on 26-06-2025

INTRODUCTION

Chalcones principally belong to the class of flavonoids in the plant kingdom (Li *et al*., 2024a). Chalcones consist of two fragrant rings namely, ring A and B, which contain various orders of substituents and are alpha, beta unsaturated ketones. In Chalcones, three aliphatic carbon series connect two fragrant rings. Those plants which contain chalcones have been employed as therapeutic remedies across the Balkan countries. To name a few, these plants are *Ruscus*, *Angelica*, *Piper,* and *Glycyrrhiza* (Krishna *et al*., 2024). Lico chalcones, which are isolated from the plant of liquorice, possess multiple biological activities; for example, antimalarial, chemopreventive, antispasmodic, anti-fungal, antioxidant, anti-bacterial, and anti-tumor (Jose *et al*., 2024). An ample quantity of dihydrochalcones and chalcones are found in apples and sour fruits. Furthermore, these complexes can formulate a better addition to the total daily usage of organic or unrefined polyphenolic compounds apart from research flavonoids (Asadzadeh Bayqara *et al*., 2024). The treatment of inflammatory diseases mainly relied upon the targeting of the cyclooxygenase enzyme, and towards this end, several bioactive compounds, including both synthetic and natural have been discovered. Another approach targets suppression of the inflammatory mediators such as Prostaglandin E2 (PGE2) and Nitric oxide (NO), which are implicated in upregulating the inflammation.(Marchon *et al*., 2024). Nuclear factor kappa B (NF-κB) is a transcription factor that plays a key role in inflammatory responses through the induction of several pro-inflammatory genes, including those encoding chemokines, cytokines, and adhesion molecules. Interestingly, Chalcones and their derivatives have shown the potential to suppress NF-κB and offer an anti-inflammatory therapeutic approach (Siddiqui *et al*., 2024).

Arisaema utile belongs to the family *Araceae*. The genus *Arisaema,* belonging to the family of *Araceae,* is used for food and medicinal purposes by human populations. Different plants belonging to the Arisaema genus are used to treat various ailments. A variety of plants belonging to the genus *Arisaema,* exhibit different activities, i.e., anti-bacterial, cytotoxicity, anti-fungal, anti-microbial, anti-oxidant, anti-allergic, anti-tumor, and insecticidal. Traditionally, different plants of the genus *Arisaema* have been used for the treatment of various diseases such as cough, asthma, cold, dampness, etc. Several phytochemicals, such as flavonoids, glycosides, saponins, alkaloids, and tannins, etc. have been isolated from *Arisaema* plants. However, the therapeutic potential of chalcone derivatives (Utilito) isolated from *Arisaema utile*, particularly in relation to Alzheimer's disease, remains largely unexplored. The present study aims to isolate and characterize a novel chalcone from *Arisaema utile*, and to investigate its potential as a selective MAO-B inhibitor through molecular docking studies. By evaluating its binding affinity and interaction profile with

**Corresponding author:* e-mail: maliksaadullah@gcuf.edu.pk

AD-related enzymes, this research seeks to establish a foundational step toward the development of a new class of natural MAO-B inhibitors for Alzheimer's therapy. (Gaur and Siddique, 2024)

Alzheimer's disease (AD) is a complex neurodegenerative condition and one of the most common forms of dementia. It involves personality changes, cognitive decline, and unusual behaviors (Ravi *et al*., 2018). The exact cause of these changes is still not fully understood, but hallmark features in the brain of AD patients include the buildup of amyloid beta (Aβ) peptides and the abnormal presence of hyperphosphorylated tau (p-tau) proteins (Tarragon *et al*., 2013). Aβ accumulates as extracellular plaques known as senile plaques (SP), whereas p-tau aggregates into neurofibrillary tangles (NFTs). Additionally, AD has been linked to mitochondrial dysfunction, damage to synapses, chronic inflammation, problems with neurotransmission, hormone imbalances, and cell cycle abnormalities (Lam *et al*., 2016). Aging is the most common risk factor for AD, but genetic predispositions and environmental influences also play critical roles.

Sodium azide is commonly utilized in experimental models of AD because it inhibits mitochondrial cytochrome c oxidase (complex IV), resulting in oxidative stress, neuronal dysfunction, and energy failure (Tönnies and Trushina, 2017a; Zhang *et al*., 2021), which are significant characteristics of AD pathology. Chronic exposure to sodium azide in rats induces memory impairment, increases reactive oxygen species, and causes neurodegenerative changes, thereby serving as an appropriate agent for the induction of AD models.

Monoamine oxidases, namely Monoamine Oxidase A (MAO-A) and Monoamine Oxidase B (MAO-B), are mitochondrial enzymes involved in the oxidative deamination of neurotransmitters (Behl *et al*., 2021a). MAO-B is upregulated in aging and AD brains (Jaisa-Aad *et al*., 2024), significantly contributing to increased hydrogen peroxide levels and neuronal damage. MAO-A plays a role in neurochemical regulation and is associated with the progression of neurodegenerative diseases. Inhibition of these enzymes, especially MAO-B, has demonstrated a reduction in oxidative stress and enhancement of cognitive outcomes in preclinical studies of AD (Alborghetti *et al*., 2024).

The phytochemical and bioactivity profiling of *Arisaema jacquemontii* revealed high antioxidant potential (87.66% DPPH scavenging), alongside significant cytotoxicity against DU-145 and HL-60 cancer cell lines, further underscoring the therapeutic effects of this *Arisaema* (Tabassum *et al*., 2019). Additionally, *Arisaema* species show remarkable resistance to free radical-induced oxidative stress. *Arisaema propinquum's* methanolic leaf extract greatly inhibited free radicals. The methanolic leaf extract exhibited an IC_{50} of 0.563 ± 0.50 mg/ml for DPPH, 1286 mM Fe^{2+}/mg extract for FRAP, an EC50 of 1.66 ± 0.18 mg/ml for reducing power, and a chelation capacity of about 51% at 100 µg/ml (Bibi *et al*., 2011). The antioxidant potential of *Arisaema* cum Bile's aqueous extract was investigated, showing its ability against free radicals using tests for hydroxyl radicals (59.62%), hydrogen peroxide (98.13%), and DPPH (90.63%). The methanolic extract isolated from *Arisaema*. *tortuosum* tubers possess anti-inflammatory effects, with 86.20% inhibition of diene-conjugate synthesis and 92.92% suppression of beta-glucuronidase enzyme activity (Du *et al*., 2011). Based on these therapeutic effects, we isolated and characterized a novel chalcone derivative (utilito) from *Arisaema utile* to investigate its neuroprotective, antioxidant, and MAO-B inhibitory activities in a sodium azide-induced rat model of AD.

The benzimidazole-chalcone derivatives were synthesized and screened for monoamine oxidase (MAO) inhibitory activity. Most compounds demonstrated stronger inhibition of MAO-B than MAO-A. Notably, compound BCH2 exhibited the most potent MAO-B inhibition, with an IC_{50} of 0.80 µM, and showed the most potent MAO–B inhibition among all. The BCH4 followed BCH2 with an IC_{50} of 1.11 µM for MAO-B inhibition (Krishna *et al*., 2023). According to these findings, utilito may have a potent MAO-B inhibitory effect and may be useful in treating neurodegenerative disorders like AD.

MATERIALS AND METHODS

Plant collection

Whole plant of *Arisaema utile* was collected from Iwan Patti, natthal top Muzaffarabad, and a voucher specimen MUH- 4453 was deposited in the herbarium for future reference.

Plant extraction

The maceration technique was used for the preparation of plant extract as described previously. (Saadullah *et al*., 2024).The Results of extraction are shown in table 1.

Chemicals, equipment's and solvents

Chloroform, Ethanol, n-hexane, ethyl acetate, dichloromethane, thin layer chromatography (TLC) silica gel plate 60 F_{254} were used for extraction and isolation. For the visualization purpose of different components under UV light at shorter wavelength (254nm) and longer wavelength (366nm), 10% sulphuric acid and godine reagent were used as spraying agents. To isolate different compounds, column chromatography (mesh along with Sephadex LH-20 with silica gel of 70-230, 230-400) was used. To determine ultraviolet spectra Lambda-25 spectrophotometer (Perkin Elmer) was used. The 13C-NMR spectra were developed using the same instrument as the 1H-NMR at 150 MHz and 100 MHz. The Hetero nuclear single quantum coherence (HSQC) and Heteronuclear multiple bond correlation (HMBC) spectra

were also acquired at 600 MHz and 500 MHz. Both Finnegan MAT 312 and MAT 311 were used for field desorption, recording Electron ionization mass spectroscopy (EIMS) with the data system of Mass Pec, for field ionization and Peak matching, respectively. High-resolution mass spectroscopy (HRMS) was performed by Joel JMS (HX 110) MS.

Preliminary screening of secondary metabolites

Finely powdered plant extract was taken and then weighed accurately. According to the standard procedure, different phytochemical tests were carried out for secondary metabolites. Dragendorff's, Wagner's, and Mayer's reagents were used for alkaloid screening. Salkowski's and Keller Kiliani test was used for cardiac glycosides, while Borntrager's test was used for modified anthraquinones. The froth test is used to identify saponins, whereas the gelatin, catechin, and ferric chloride tests were used to screen for tannins. Lead acetate, sulfuric acid, and alkaline reagent tests were conducted for flavonoids (Savithramma *et al*., 2011).The results of preliminary screening metabolites are shown in table 2.

Isolation of novel compound

While the column chromatography was being used with silica gel 60 (63-200 μm) as the stationary phase and chloroform, methanol, water (80:20:2) as the mobile phase during a stepwise elution method with increasing polarity, 10 g (AUE) extract of *Arisaema utile* was fractionated. Then the six fractions (AUE 1-6) were obtained. After that, the fraction AUE 4 of 3.75 gm was selected on the basis of thin-layer chromatography. Column chromatography was performed using silica gel 60 of 40-63 μm as the stationary phase and n-hexane: ethyl acetate (3:1) as the mobile phase. The six more fractions (AUE 4-a - AUE 4-f) were obtained by this process. The Size exclusion chromatography was performed with AUE 4-e of 580mg using Sephadex LH-20 as the stationary phase and pure methanol as the mobile phase. By this process, four more fractions (AUE 4e-a to AUE 4e-d) were obtained (Nguyen *et al*., 2018). Based on TLC observation, the AUE 4e-d (0.93mg) was obtained as a novel compound (utilito) which is shown in fig.1. Purification scheme of the new compound from ethanol extract of *Arisaema utile* was designed, which is illustrated in fig. 2.

Elucidation chart

C^{13}-NMR (125MHz) and ^{1}H-NMR (500MHz) spectral data of utilito was shown in table 3.

Molecular docking studies

The molecular docking analysis was performed to analyze the interaction of novel chalcone (utilito) with the target proteins. For this purpose, Autodock 4.2 was used to carry out the protein-ligand interaction analysis (Morris *et al*., 2009) . The analysis specifically focused on MAO-B, a key enzyme implicated in Alzheimer's pathogenesis, along with other related enzymes such as AChE, BChE, and MAO-A for comparative purposes.

Preparation of ligand and protein

Using Chem3D Pro, the isolated molecules were transformed into the appropriate 3D format. Research Collaboratory for structural bioinformatics (RCSB) Protein Data Bank was used to obtain the targets of protein Acetylcholinesterase (AChE) (PDB ID: 4BDT), Butyryl cholinesterase (BChE) (PDB ID: 4BDS), MAO-A (PDB ID: 2Z5Y), and MAO-B (PDB ID: 2V5Z) (Binda *et al*., 2007, Son *et al*., 2008, Nachon *et al*., 2013). Discovery Studio 4.0 was used to prepare the target proteins by removing the heteroatoms, water molecules, and ligands. Through AutoDock, Kollman charges were applied. Molecular docking was performed by setting the grid, and the lowest binding energies were calculated. The docked compounds were visualized using the Discovery Studio (Visualizer 2005.) and protein and ligand interactions were studied.

Molecular dynamics simulation studies

Utilizing Nano scale sub-atomic dynamic (NAMD) programming on a CUDA-accelerated GPU machine with a 16 center computer chip and 64 GB of RAM memory (Bowers *et al*., 2006), the atomic unique investigation of the ideal docked conformity was completed. Geography records were made for both the protein and the ligand (Kim *et al*., 2017) after the best docked protein-ligand structures were chosen utilizing the CHARMM36 force field. To return the answer for an impartial state, NaCl charges were added at a standard grouping of 0.15 M. The framework was adjusted for 500000 stages in the NVT group and afterward for 500000 extra steps in the NPT ensemble (Barclay and Zhang, 2021). The limiting energy, Vander wall forces, and electrostatic communications were resolved utilizing the PME strategy (Guckel, 1999).

Enzyme assays

The action of recombinant human MAO-A and MAO-B was measured utilizing kynuramine (0.06mM) and benzylamine (0.3mM) as substrates, separately. Electrophorus electricus Type VI-S was utilized to gauge the activities of Hurt and butyryl cholinesterase (BChE) in the sight of either 0.05 mM butyryl-thiocholine iodide (BTCI) or 0.5 mM acetyl thiocholine iodide (ATCI), individually. 0.5mM, 5.5′-dithiobis (2-nitrobenzoic corrosive) (DTNB) was added. The 7-methoxycoumarin-4-acetyl-[Asn670, Leu671]-amyloid β/A4 protein part 667-676-(2,4-dinitrophenyl) Lys-Arg-Arg amide trifluoroacetate was utilized as a substrate in a BACE-1 (BACE-1) movement identification pack to gauge BACE-1 action. BACE-1 action estimation units, synthetic substances, and enzymes such as recombinant human MAO-A and MAO-B were purchased from Sigma-Aldrich (St. Louis, MO, USA) (Finberg and Rabey, 2016) (De Colibus *et al*., 2005).

Enzyme inhibitory and kinetic studies

At a portion of the value of 10 µM, novel compound inhibitory impacts against MAO-A, MAO-B, Throb, BChE, or BACE-1 were first evaluated. Subsequent to deciding the mixtures' half maximal Inhibitory concentration (IC_{50}) values for MAOA and MAO-B, compounds having lingering action under half were inspected for their impacts on Throb, BChE, and BACE-1 45. As recently announced, motor tests were performed on the components of PC10 and PC11, that was restrained MAO-B, at three inhibitor focuses (Ramsay and Albreht, 2018) and five substrate fixations.

Inhibitor reversibility analysis

After preincubating PC10 and PC11 at 0.15 µM with a MAO-B for almost 30 minutes, as recently portrayed, the reversibility of their MAO-B hindrances was assessed by dialysis. Lazabemide, a reference reversible MAO-B inhibitor, and pargyline, a reference irreversible MAO-B inhibitor, were preincubated with MAO-B at 0.20 and 0.30 µM, respectively, for correlation. Lazabemide and pargyline were purchased from Sigma-Aldrich (St. Louis, MO, USA). By differentiating the movement of dialysed (Promotion) and undialyzed (AU) tests (Rojas *et al*., 2015), reversibility designs were assessed (Rojas *et al*., 2015).

Ethical approval

Ethical considerations were taken into account as ethical approval (Reference no. GCUF/ERC/2077) was sought before the start of the study. The approval was taken from the Institutional Review Board of the Government College University, Faisalabad, and it is approved by the Institute of Laboratory Animal Resources, Commission on Life Sciences, University, National Research Council (1996).

Animals

For *in vivo* studies, wistar rats (250-300 g, 10-12 weeks old) were procured from the University of Agriculture, Faisalabad, Pakistan. The animals were acclimated for seven days in the Government College University Faisalabad animal facility, the temperature was maintained at 23 ± 2 °C under the supervision of 12-hour light/dark cycle, and they were provided the required access to water and food (Saadullah *et al*., 2024).

Experimental model of Alzheimer's disease

Sodium azide was used to induce AD in Wistar rats as the six groups were made for the division of rats having n=6. Using the dose of 12.5 mg/kg, it was administered intraperitoneal for the first 5 days, later 10 mg/kg was given for nine days. The novel chalcone was administered at day 15 for two weeks. The novel chalcone was administered at the doses of 100 mg/kg, 200 mg/kg, and 300 mg/kg into three respective groups. Rivastigmine was used as a standard and administered similarly to the novel chalcone. For the control group, distilled water was administered at a dose of 1mL/kg (Singla *et al*., 2022). The experimental model of alzheimer's disease, as illustrated in fig.3.

Behavior studies

Morris water maze tests

A plastic tub was used with 1.5 feet and 1m diameter. Tap water was used to fill the tub at 26°C. A platform was placed at the center that was one inch below the surface of the water. The pool was divided into four halves and named as N, S, E, and W (north, south, east, and west, respectively. During the habituation period, the rat was guided to the platform, while on trial day (6^{th} day), the rat was not guided to the platform, nor was the platform visible to the rat. The rat was videotaped on trial day for 2 minutes to reach the platform. The time the rat took to reach the platform was recorded.

Open field test

The open field apparatus for behavioural assessment was utilized by Saleem, *et al*. (2022). The apparatus constructed from 72 × 72 cm plywood with 36 cm high walls, resembling a square tank painted with white resin. Each rat was gently placed in a corner of the arena, and its movements were recorded over a 10-minute session. Parameters measured included the number of lines crossed with all four paws, stretch postures, total distance travelled, with passing time in the central area, *fecal boli* count, developing behaviours, raising frequency, and freezing moments. This setup aligns with established protocols for evaluating rodent exploratory and anxiety-related behaviours.

Y-maze test

The test was performed according to Akhter et al. (2025)**.** The apparatus utilized consists of three wooden arms linked at 120^{o} to each other in the Y shape. The apparatus arms were 25 cm tall, had a length of 35 cm, with a triangular midway zone, and a width of 10 cm. The exploratory behavior of animals in the Y-maze was videotaped for eight minutes. Arm was observed, and when the back paws were completely entered into the arm, that infiltration was deemed acceptable for that duration.

Estimation of biochemical parameters

Preparation of tissue homogenate

Under mild anesthesia, many animals were sacrificed, and for results, the brain from every rat under investigation was excised with meticulous care post cervical dislocation. The brains, isolated from rats, were eventually washed with normal saline to remove blood; they were then preserved at a temperature of -80 degree centigrade. Brain samples were homogenized in 0.1 M phosphate buffer *PH 7.4* to generate tissue homogenates; these included 1 mM Etylenediamine tetracetate (EDTA), 0.25 M sucrose, 1 M Phenylmethylsulfonyl fluoride (PMSF), and 1 0 mM KCl. The mixture was then centrifuged at 800 rpm for half an hour at a temperature of 4 degrees centigrade to get supernatant (Lakshmi *et al*., 2015).

Estimation of catalase (CAT) activity

In order to carry out the experiment, the reaction mixture consisted of 1.95 mL of phosphate buffer (pH 7.0, 50 mM), 50 µL of brain homogenate, and 1mL of 30 mM H_2O_2. The activity of catalase was determined by gauging optical density at 240nm (Goldstein, 1968). It requires a three-time repeat.

Estimation of superoxide dismutase (SOD) activity

In order to form a reaction mixture, the tissue homogenate (100 µL), phenazine methosulfate (100µL) nitro blue tetrazolium (300 µL), Triton X (200 µL) were mixed with 1.2 mL of sodium phosphate buffer (0.052 M, pH 8.3). By incubation of the solution at 30 degrees for the ninety-five seconds, to stop the chemical reaction, specifically the glacial acetic acid was precisely mixed. By doing centrifugation at 1000 rpm, the n-butanol surface layer was separated on one side; the n-butanol was then utilized as a blank, and eventually, chromogen and its intensity were measured at 560 nm. The procedure again requires repetition three times for better results. (Kakkar *et al*., 1995).

Estimation of reduced glutathione (GSH) level

The experiment needs 1 milliliter of KCl and 1 milliliter of tissue homogenate, along with 4 milliliters of cold refined water. The mixture was then treated with 1 milliliter of trichloroacetic acid and it was then centrifuged for half an hour at 3000 rpm. 0.1 mL was then mixed with Tris-buffer (0.4 M), 0.001M and 4 mL of DTNB 2 mL of precipitation. The absorbance capacity for the blank and sample formed with all reagents other than brain homogenate was determined at 412 nm (Saleem *et al*., 2019). The previous process will be repeated three times for the eventual results.

Estimation of malondialdehyde (MDA) level

In this examination, oxidative stress and lipid damage mediated free radical levels were measured. One milliliter of TBA 0.38% (w/w), one milliliter of hydrochloric corrosive (0.25 M), and one milliliter of 15% (trichloroacetic corrosive) were consolidated to make what is known as the TBA reagent. To 3 mL of TBA reagent that had been created, 1 mL of an aliquot of the homogenized sample was added. After about 15 minutes of hatching, the response blend was cooled in an ice water shower and centrifuged for 10 minutes. Absorbance was estimated at 512 nm after the supernatant was gathered. $MDA = Abs \times 100 \times Vt/1.56 \times 105 \times Wt \times VU$

Where *Vt* total volume of the mixture, *Wt* weight of the hippocampus, and *Vu* is the volume of the aliquot used.

STATISTICAL ANALYSIS

The data was examined in the form of mean ± SEM, and one way and two-way ANOVA (Bonferroni post hoc test) was utilized to investigate the data by utilizing the Graph Pad Prism 5.01 version (USA). A p-value < 0.05 is reflected as statistically significant.

RESULTS

Antioxidant activity of novel chalcone (Utilito)

DPPH scavenging activity was used to express antioxidant activity, and it consistently increased as sample concentration increased (table 4 and fig. 4). A sample containing 350 µg/ml exhibited DPPH scavenging activity of up to 71 ± 0.11%. Using DPPH activity for removing impurities to estimate in vitro antioxidant potential. The *in vitro* antioxidant capacity of compound (utilito) was assessed using the DPPH scavenging assay; the results are shown in table 5. The DPPH scavenging activity was also used to assess the *in vitro* antioxidant potential of ascorbic acid, which was shown in fig 5.

Behavioral studies

Morris water maze test

In the plate form quadrant, swim timing is inversely proportional to memory impairment. As compared to the other groups, the swimming time of rats treated with sodium azide was significantly decreased. The standard group showed the greatest spatial learning with a highly significant difference. However, groups administered with different doses of novel chalcone (utilito), such as 100, 200, and 300 mg/kg, showed a similar improvement in cognitive abilities. Three groups treated with the novel chalcone increase in swimming time with dose dose-dependent impact. Impact of novel chalcone (Utilito) on the Morris water maze test for memory reduction in rats (fig.6)

Open field test

A decline in horizontal square crossing and rearing was considered proportionate to a decline in locomotor and cognitive ability. The movement and cognitive capacities of sodium azide-treated rats were significantly less. When compared to the group treated with the sodium azide, variation for all other groups was high ($P < 0.001$). Rats in the standard group had better arena exploration.

A dose-dependent increase in exploring rearing and movements was observed in the group treated with novel chalcone (100, 200, and 300 mg/kg). Table 6 shows that utilito improved locomotor activity and reduced anxiety in the AD model, suggesting neuroprotective effects

Y maze test

The % age alteration exhibited the result of spatial learning as well as cognitive abilities. The group treated with sodium azide exhibited the lowest % age of alteration, which reflects the severe deterioration in spatial learning when compared with all othergroups ($P < 0.001$). Utilito (100 mg/kg) group and the Standard group gave comparable values of % age alteration with the control group. Novel chalcone (Utilito) dose 300 mg/kg group expressed maximum % age alteration, ($P < 0.001$) in comparison to control group and the results are given in table 7.

Biochemical parameters in brain oxidative stress biomarkers

The oxidative stress biomarkers were measured after induction of Alzheimer's disease with, sodium azide to assess the anti-oxidant enzymatic activity in rat brain tissue. The activity of anti– oxidant enzyme and GSH level in the brain tissue, are closely connected AD. Recovery CAT activity, MDA activity, SOD, and GSH content were examined as illustrated in fig 7.

Molecular docking

AChE

Amino acids such as PRO446, TRP439, TYR337, TYR449, THR83, TYR341, SER125, TRP86, ASN87, and GLN71 were implicated in interactions, both bonding and non-binding, with utilito. The amino acids TYR341, THR83 made a Carbon-hydrogen interaction with the 1,2-dimethoxybenzene ring. The amino acid involved in non-bonding (hydrophobic) interactions was: PRO446, TRP439, TYR337, as shown in fig 8

BuChE

TRP430, TYR440, TRP82, HIS438, GLY116, SER198, PHE329, PRO285, SER287, LEU286, TRP231 amino acids were implicated in interactions, both bonding and non-binding with compound (utilito). The dihydro-pyrrole ring made conventional hydrogen bond interactions with amino acids TRP86, ASN87. The amino acids GLY116, SER198 made a Hydrogen bond interaction with the double-bonded oxygen between the phenol and dimethoxybenzene ring. The amino acids HIS438, TRP82 made a pi-pi T shaped interaction with the 1, 2-dimethoxybenzene ring as shown in fig 9

MAO-A

The amino acids such as PHE352, VAL303, VAL65, CYS406, GLY67, GLY66, LYS305, TYR407, ARG51, ASN181 were implicated in interaction, both bonding and non-binding with the compound (utilito). The dihydro-pyrrole ring made pi-sulphur interaction with CYS406. The amino acid hydrogen bond interaction with ALA68, TYR69, with the double-bonded oxygen between the phenol and the dimethoxybenzene ring. The amino acid ASN showed a hydrogen bond interaction with the pyrrole ring, as shown in fig 10

MAO-B

The amino acids such as PRO104, PHE103, LEU164, TRP119, LEU167, ILE316, ILE199, CYS172, ILE198, LEU171, TYR398, TYR435 were implicated in interactions, both bonding and non-binding with the compound (utilito). The dihydro-pyrrole ring made Conventional hydrogen bond interactions with amino acids LEU171, TYR398, and TYR435 with the phenol ring, respectively. The amino acid ILE199 made a pi-sigma interaction with the 1,2-dimethoxybenzene ring. The nonbonding interaction included amino acids: ILE316, CYS172, ILE198 as shown in fig 11

Molecular dynamics simulations

Simulation results of AChE

To assess the molecular dynamics and stability of the acetylcholinesterase (AChE) protein complexed with ligand (utilito), we conducted a simulation under periodic boundary conditions using 50-nanosecond molecular dynamics (MD) in an aqueous environment. Both the unbound AChE protein and its complex with utilito served as initial configurations for the MD simulations. We employed the CHARMM36 force field to generate parameter files for the protein and ligand, immersing the system in a TIP3P water model. To evaluate system stability, we calculated for both the protein and its complex, the Root Mean Square Deviation (RMSD) and Root Mean Square Fluctuation (RMSF). RMSD analysis focused on the backbone atoms, comparing deviations from initial conformations. A complex is considered stable if its average RMSD remains below 5.0 Å over the simulation period. The fig. 13 shows the RMSD for the protein and its complex. Our results, depicted in fig. 12, show that the unbound AChE protein maintained an average RMSD of 2.5 Å for the first 30 ns, with minor fluctuations thereafter. The AChE-utilito complex exhibited initial variations but stabilized after 5 ns, indicating robust stability in the aqueous medium.

Further insights were obtained through RMSF analysis, which measures the flexibility of individual amino acid residues over the simulation period. As shown in fig. 13, the C_α atoms of most residues in both the unbound AChE and its complex with utilito displayed fluctuations of less than 4.0 Å. Notably, terminal residues exhibited higher fluctuations, likely due to their exposure and flexibility. The ligand 1a also showed some fluctuations, suggesting dynamic interactions at the binding site. These RMSF findings corroborate the stability of both the protein and its complex in an aqueous environment.

Simulation results of MAO-B

Similarly, for the 2nd protein, molecular simulation was run with ligand 1a. On the pattern of the previous protein, a simulation was carried out for the MAO-B complex under similar conditions. Both the protein and its corresponding complex were found out as stable having RMSD value below 3 A. Both protein and its corresponding complex, and their RMSD, are shown in fig 14**.** Initially, both MAO-B and its complex, along with their RMSD and utilito, displayed continuous instability, however, they became stable after five minutes for an average RMSD of 2.65 A. At the final point of simulation after 40ns, the RMSD value of the protein ligand complex showed shakiness and variations; however, the available data clearly demonstrated the protein and its corresponding complex in a stable condition in aqueous media.

2nd ligand -protein complex and RMSF analysis was carried out with results presented on the fig. 15. The RMSF for Ca atoms, the great majority of amino acids,

residual elements of VEGR2, protein, and its complex, along with utilito, showed less than 3.0 A. All of the residues are extremely stable, especially terminal residues of protein expressed relatively utilito more stability with low RMSF value; the phenomenon could be associated with the compressed nature of protein. The data of RMSF presented stability both in protein and its complexes in an aqueous environment.

DISCUSSION

Alzheimer's disease (AD) is a chronic, gradually degenerative neurologic disorder that affects millions of people worldwide. It is mainly characterized by a decline in cognition, such as memory impairment, impaired learning, and progressive loss of independent functioning.

Consequently, patients with AD suffer from a decline in their capacity to carry out daily activities, with increasing needs for care at higher stages of the disease. The disease is the biggest clinical and public health threat of the 21st century, driven by an increasingly aging population, resulting in a sharp rise in its prevalence (Castellani *et al*., 2010). Therefore, with an aging global demographic set to contribute an even greater burden for the coming decades, it makes the urgency to find effective treatments is more crucial than ever. Current drug therapies against AD, such as cholinesterase inhibitors and glutamate regulators, are only symptomatic and temporarily improve or stabilize symptoms with no cure currently (Li *et al*., 2022, Lin *et al*., 2021). Clearly, there is an urgent need to explore the development of new, much more effective therapeutic interventions to impede or halt further progression of the disease and its disastrous consequences. Pathogenesis of AD is multifactorial and complex, with several contributing factors that interact intricately.

The key pathological features of Alzheimer's disease include deposition of amyloid-beta plaques, tangles of tau, mitochondrial dysfunction, oxidative stress, and neuroinflammation (Lim *et al*., 2021, Ekundayo *et al*., 2021). These lead to disruptions in normal neuronal activities as well as communication pathways, eventually translating into neuronal death with progressive cognitive degradation. The latest studies emphasize the very important role oxidative stress and neuro inflammation play in the pathogenesis and development of AD. Oxidative stress is defined as an imbalance between the excessive production of reactive oxygen species and the ability of the body to neutralize such harmful molecules with antioxidants (Firdous *et al*., 2024, Gao *et al*., 2014). The result is cellular damage, neurodegeneration, and the degradation of brain tissue. Meanwhile, neuroinflammation, which is due to the responses of microglia and astrocytes, further exacerbates neuronal damage. This results in pro-inflammatory cytokines and other damaging mediators that cause more deterioration in the brain, thereby accelerating the progression of the disease. Thus, the cross-talk of oxidative stress and neuroinflammation underlines these elements as key targets for future therapeutic interventions to halt or delay the progression of Alzheimer's disease (Dhapola *et al*., 2024, Agostinho *et al*., 2010). Our research was aimed at evaluating the neuroprotective activity of a recently isolated chalcone derivative (utilito) from *Arisaema utile*, but focusing particularly on its expected to be as an inhibitor of monoamine oxidase B (MAO-B). An MAO-B inhibitor would be highly useful since neuroinflammation and oxidative stress play the significant role in pathology of Alzheimer's disease (Siddiqui *et al*., 2023). This chalcone derivative (Utilito) seems to be an effective compound in alleviating both oxidative damage and neuroinflammation that have previously been positively linked to Alzheimer's pathology. Since it is an MAO-B inhibitor, this compound has the potential for reducing harmful levels of ROS, therefore being a novel approach to the management of oxidative stress and its effects. In this study, the results are provided with strong evidence that has the potential to show the practical use of this chalcone derivative (Utilito) as a therapeutic agent in treating Alzheimer's disease thus advancing more targeted and effective treatments for such a debilitating condition (Behl *et al*., 2021). The inhibitory effect novel chalcone on AChE was examined. and novel chalcone showed inhibitory effect on AChE with the value of 37.4 µM at IC_{50} (µM) as shown in table 8 MAO-B is an essential enzyme involved in the breakdown and regulation of the levels of neurotransmitters in the brain, especially those involved in dopamine, serotonin, and phenylethylamine. MAO-B's principal purpose is to break down catabolic products of these neurotransmitters that would otherwise form and accumulate at inappropriate levels, affecting neural processes.

Recent studies have started linking MAO-B activity to Parkinson's disease, Alzheimer's disease, several neurodegenerative disorders, and the system of atrophy, among others, with its main task defined as the regulation of neurotransmitter levels (Chen *et al*., 2020). These results are of great importance since MAO-B activity might play the major role not only in the regulation of neurotransmitters but also in the pathophysiology of these destructive diseases. Enhanced MAO-B activity is associated with major consequences in AD. Increased enzyme activity can produce high levels of ROS, which are reactive molecules that may cause oxidative damage to the brain cells. (Wang *et al*., 2014). Consequently, targeting MAO-B activity is seen as a promising therapeutic strategy to reduce oxidative damage and slow disease progression. Our study investigated the potential of a novel chalcone derivative as an MAO-B inhibitor and showed a selective and strong inhibition of MAO–B with an IC50 of 1.37 µM against MAO-B as shown in table 9, and the results suggest that this compound is highly effective in this role (Li *et al*., 2024b).

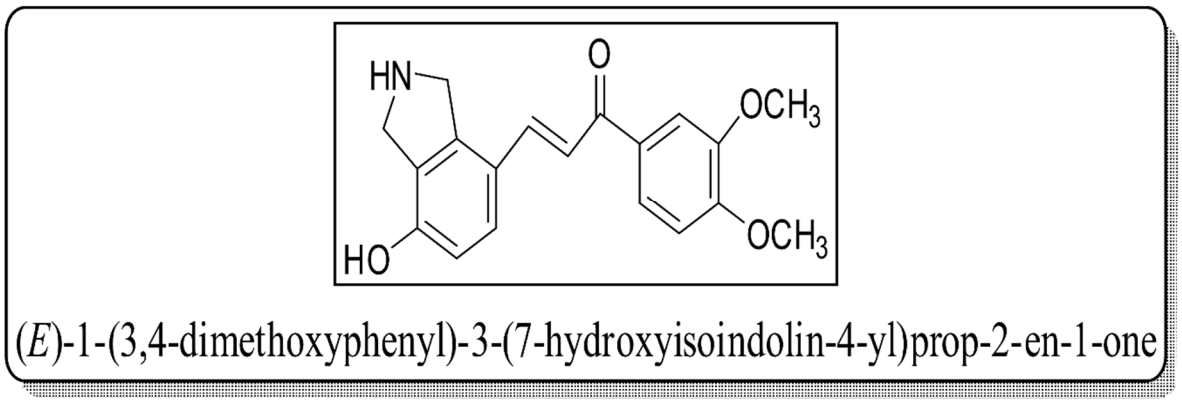

Fig. 1: Chemical structure of novel chalcone (Utilito)

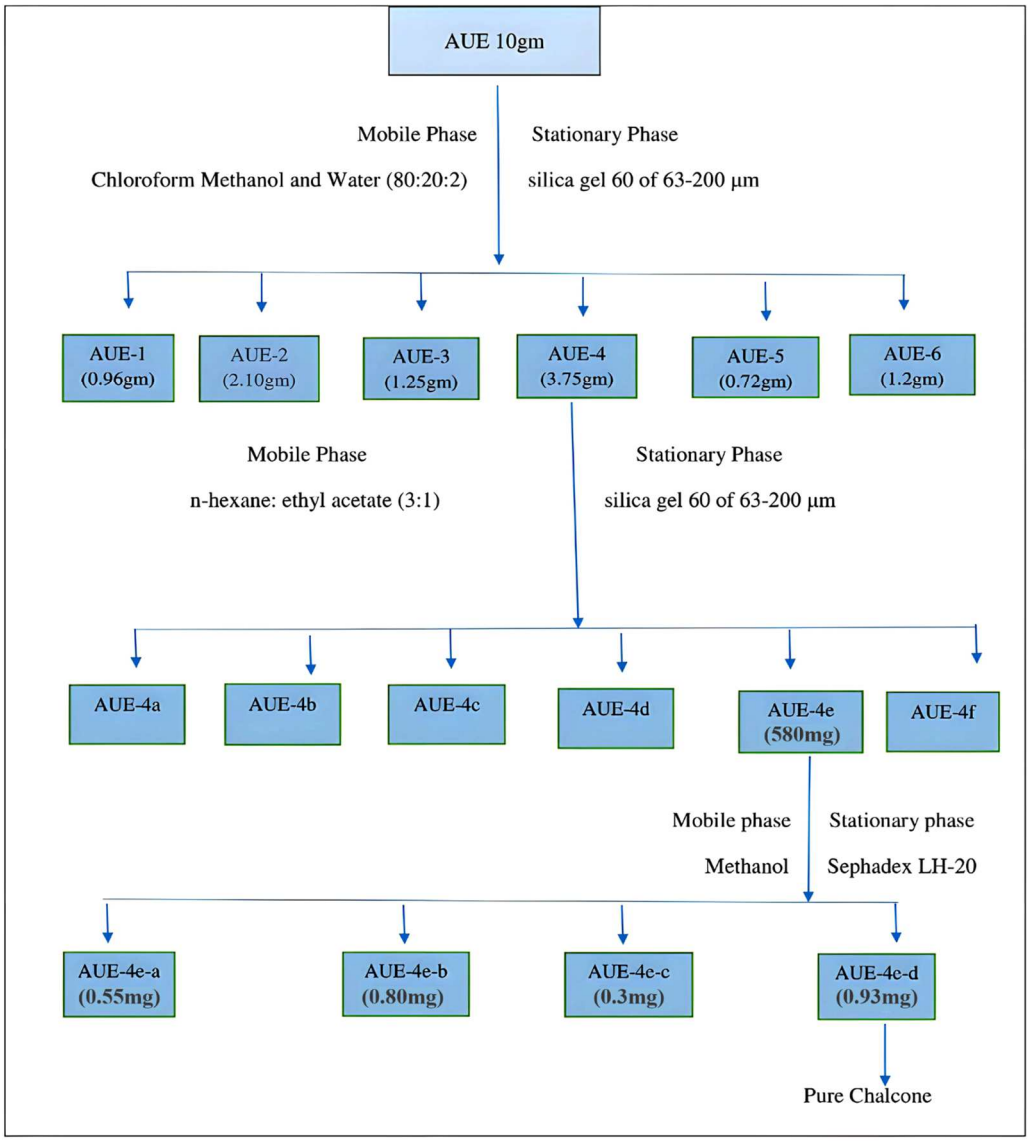

Fig. 2: Purification scheme of novel chalcone from the ethanol extract of *Arisaema utile.*

Table 1: Results of the extraction of *Arisaema utile*

Plant name	Part used	Solvent	Weight ofextract (g)	Abbreviationfor the extracts
Arisaema utile	Aerial parts (800 g)	n- hexane	08	AUAN
		Ethanol	12.3	AUAE
	Rhizome (500 g)	n- hexane	4.60	AURN
		Ethanol	9.72	AURE

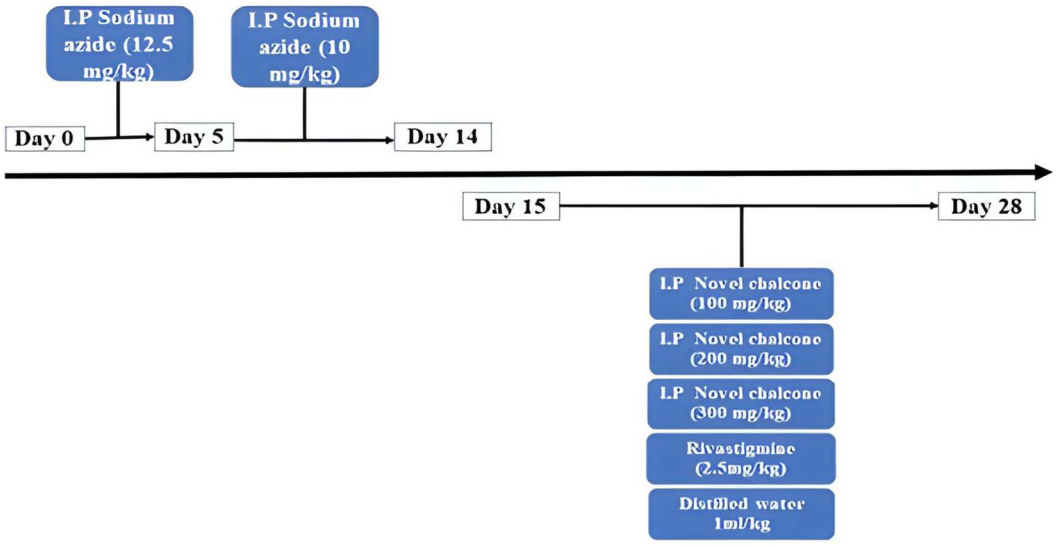

Fig. 3: Experimental model scheme of Alzheimer's disease

Table 2: Results of phytochemical screening of *Arisaema Utile*

Name of plant	Alkaloid	Anthraquinone	Cardiac glycosides	Tannins	Saponins	Flavonoids
Arisaema Utile	+	+	+	+	-	+

Table 3: Elucidation Chart. C^{13}-NMR (125MHz) and ^{1}H-NMR (500MHz) spectral data of utilito

C-No.	Multiplicity DEPT	13C-NMR	1H-NMR	J-value
C-1	-C	123.9	-	
C-2	-CH	107.1	7.33	2.11
C-3	-C	150.3	-	-
C-4	-C	155.6	-	-
C-5	-CH	112.3	7.18	1.87
C-6	-CH	105.3	7.67	1.88
C-7	-C	122.5	-	-
C-8	-CH	121.3	7.42	0.76
C-9	-CH	141.2	8.33	0.84
C-10	-C	127.5	-	-
C-11	-C	135.2	-	-
C-12	-C	123.9	-	-
C-13	-C	150.6	5.35	-
C-14	-CH	113.9	7.01	1.27
C-15	-CH	125.9	6.90	1.21
C-16	-CH2	51.1	3.81	2.14
C-17	-CH2	47.1	3.81	1.90

Table 4: Concentration to absorbance ratio of novel chalcone (Utilito)

Concentration mg/ml	Absorbance at 700nm	
	Ascorbic Acid	Novel chalcone (Utilito)
0.05	0.117	0.101
0.1	0.119	0.104
0.15	0.135	0.109
0.2	0.142	0.115
0.25	0.165	0.127
0.3	0.172	0.140
0.35	0.190	0.157

Table 5: Application of DPPH scavenging activity to assess the *in-vitro* antioxidant potential.

Concentration(µg/ml)	% inhibition of Ascorbic acid	% inhibition of novel chalcone
50	48 ± 0.26	24 ± 0.011
100	54 ± 0.12	33 ± 0.015
150	59 ± 003	40 ± 0.034
200	64 ± 0.41	52 ± 0.012
250	70 ± 0.02	59 ± 0.020
300	74 ± 0.010	62 ± 0.025
350	82 ± 0.02	71 ± 0.11

Table 6: Effect of novel chalcone (Utilito) on open field test in SA induced AD model

Groups	Total lines crossed	Time spent in central area (sec)
Control	20.09±0.587***	50±0.573***
Disease control (Sodium azide)	8.81±0.577	5.5±0.578
Standard (Rivastigmine)	25.67±0.567***	49±0.577***
Novel chalcone (Utilito)100 mg/kg	15.23±0.587***	21.23±0.567***
Novelchalcone (Utilito) 200 mg/kg	18.91±0.577***	31.57±0.587***
Novel chalcone (Utilito) 300 mg/kg	22.69±0.587***	49.81±0.577***

Number of lines crossed, Values are expresses as mean ± SEM, (n=6), *** ($p<0.05$) as compare to disease control

Table 7: Effect of novel chalcone on Y-maze test in SA induced AD model

Groups	Total no. of arm entries	Total no. of triads	Percentage alterations
Control	11.2±0.57735***	3.0±0.0**	38.33±0.5***
Disease control (Sodium azide)	2.526667±0.45	0.0±0.0	0.0±0.0
Standard (Rivastigmine)	11.3±0.57735***	3.44±0.3***	37.33±0.5***
Novel chalcone (Utilito) 100 mg/kg	8.4±0.57735***	1.0±0.0ns	21.66±0.6***
Novel chalcone (Utilito) 200 mg/kg	7.73±0.45***	2.0±0.0ns	34.34±0.8***
Novel chalcone (Utilito) 300 mg/kg	16±1.53***	4.0±0.0***	37.35±0.49***

Number of lines crossed, Values are expressed as mean ± SEM (n= 6) *** ($p<0.05$) and ns (non-significant) as compared to disease control

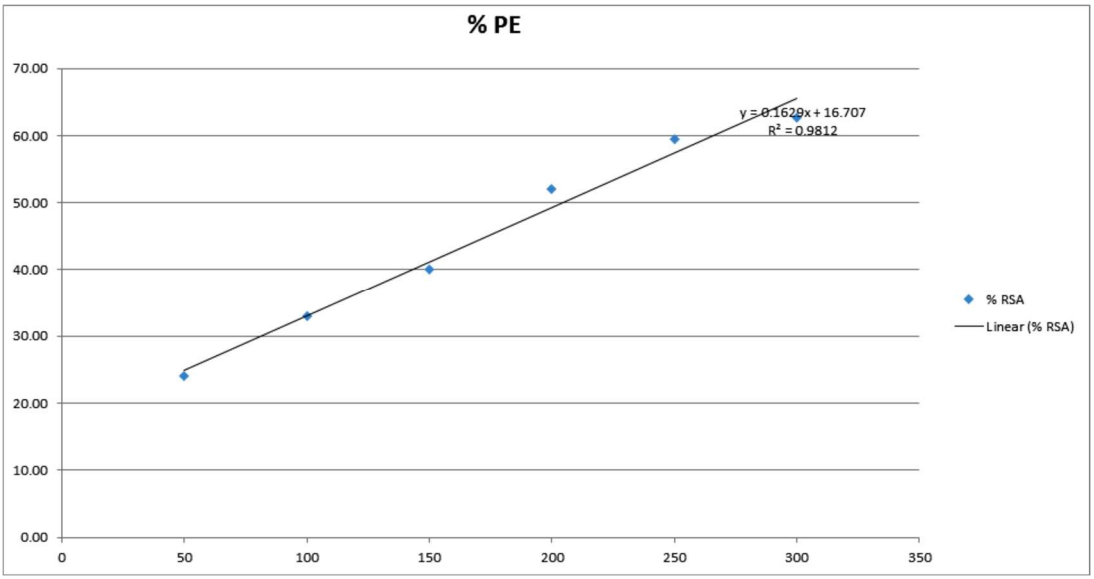

Fig. 4: Application of DPPH scavenging activity to assess the *in-vitro* antioxidant potential of novel chalcone (utilito).

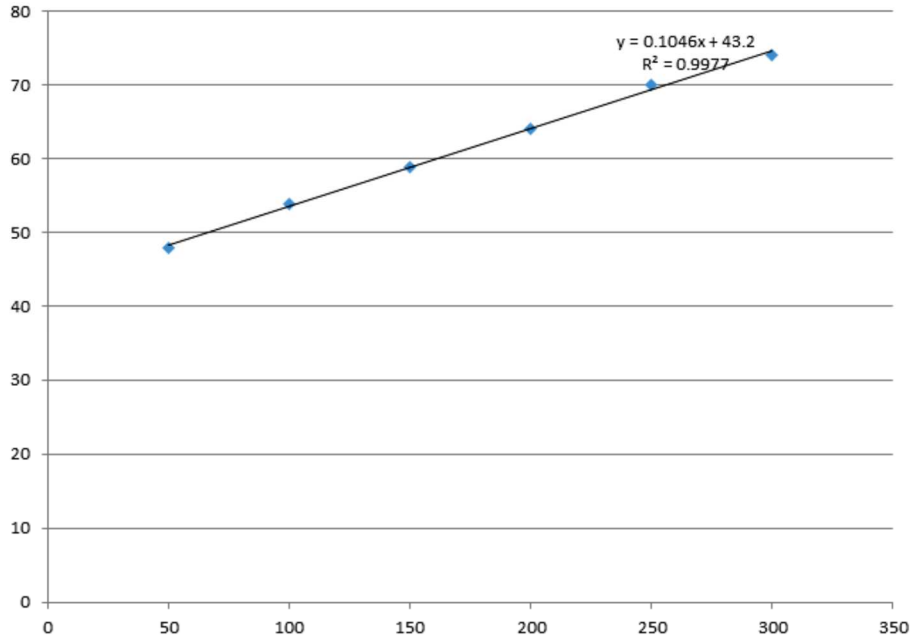

Fig. 5: Application of DPPH scavenging activity to assess the *in-vitro* antioxidant potential of ascorbic acid.

Table 8: Effect of extracts and novel chalcone (Utilito) acetylcholine esterase activity in brain tissue of AD model.

Compound/Extract	Residual activity at 10 µM (%)		IC_{50} (µM)	
	AChE	BChE	AChE	BChE
n – Haxane	43.4 ± 2.61	-	-	-
Ethanol	49 ± 1.42	-	46.6 ± 3.92	-
Novel chalcone	71.2 ± 1.07	89.1 ± 0.31	37.4 ± 2.10	-
Standard	68.4 ± 2.41	70.9 ± 0.31	26.3 ± 1.29	36.2 ± 3.65

Results are shown after the experiments in duplicate or in triplicate in reference with means ± standard errors that were carried out for precision. In order to determine values of reference compounds, they were pre incubated for half an hour with different enzyme

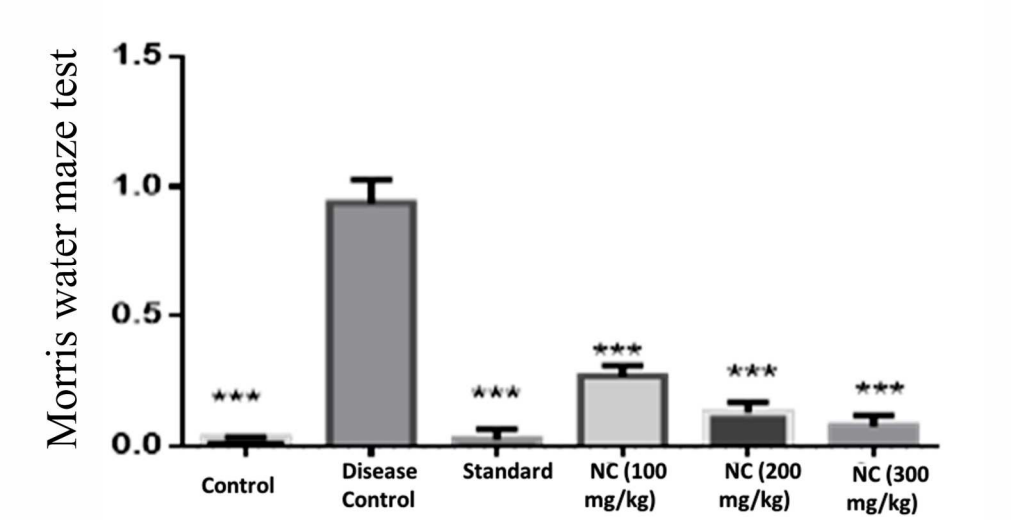

Fig. 6: Impact of novel chalcone (Utilito) on the Morris water maze test for memory reduction in rats. STD (Standard treatment): NC (Novel chalcone 100mg/kg): NC (Novel chalcone 200mg/kg): NC (Novel chalcone 300mg/kg): Values are expressed as the mean SEM, with (n=6), ** $p < 0.01$, *** $p < 0.001$ comparison to the control. Data were shown as mean. A significant *p*-value < 0.05.

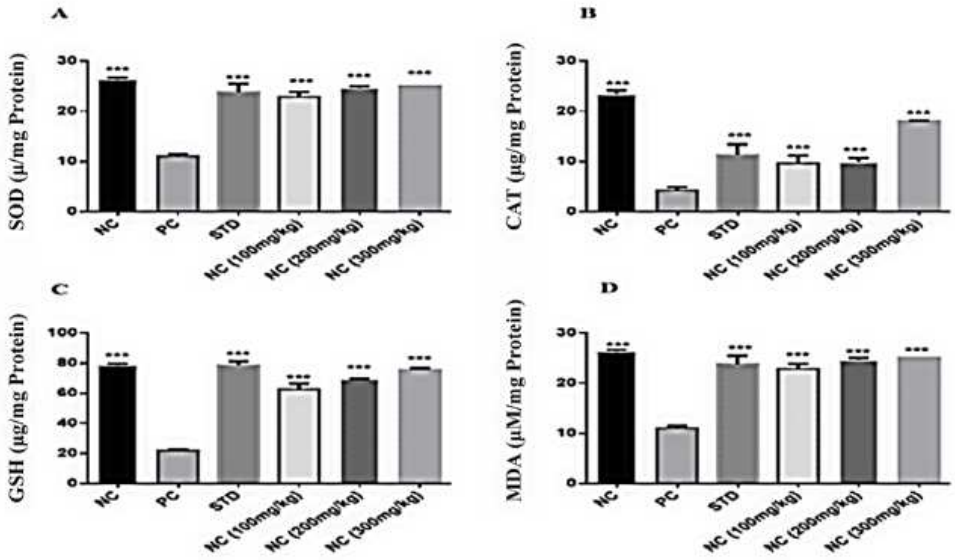

Fig. 7: Biochemical parameters (CAT, SOD,GSH and MDA) in Novel chalcone. Values are expressed as the mean SEM, with (n=6), ** $p < 0.01$, *** $p < 0.001$ comparison to the control.

Table 9: Effect of novel chalcone (Utilito) and extracts, MAO-A and MAO-B activity in brain tissue of AD model.

Compound/Extract	Residual activity at 10 µM (%)		IC_{50} (µM)	
	MAO-A	MAO-B	MAO-A	MAO-B
n – Haxane	112 ± 1.33	NA	NA	---
Ethanol	101 ± 2.11	2.31 ± 0.46	--	13.3 ± 3.14
Novel chalcone (Utilito)	99.2 ± 2.62	11.6 ± 1.17	> 40	1.37 ± 0.027
Standard	76.4 ± 1.59	13.3 ± 3.14	30.1 ± 0.14	1.56 ± 0.14

Results are shown after the experiments in duplicate or in triplicate in reference with means ± standard errors that were carried out for precision. In order to determine values of reference compounds, they were pre incubated for half an hour with different enzyme

Table 10: Docking scores of novel compound (utilito) in $kJmol^{-1}$

Code	AChE	BChE	MAO-A	MAO-B
Novel compound (utilito)	-41.2	-37.9	-40.8	-41.4

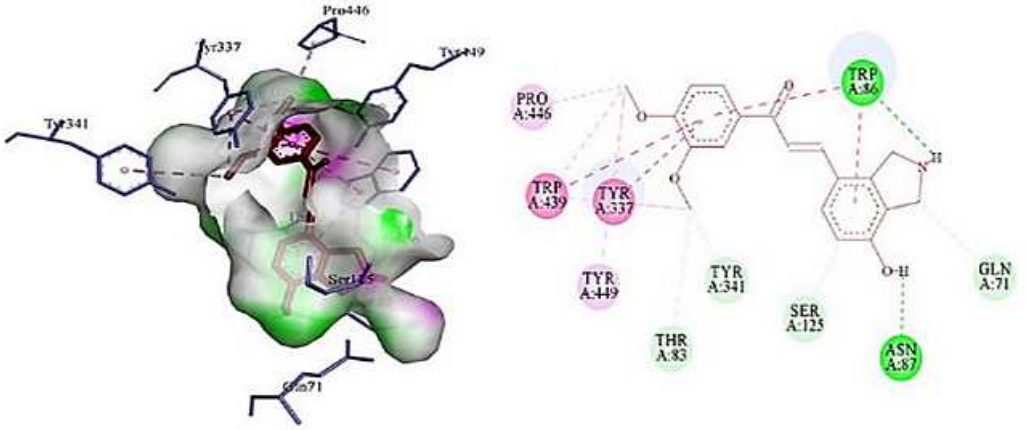

Fig. 8: 3D and 2D interactions of AChE with novel compound (utilito)

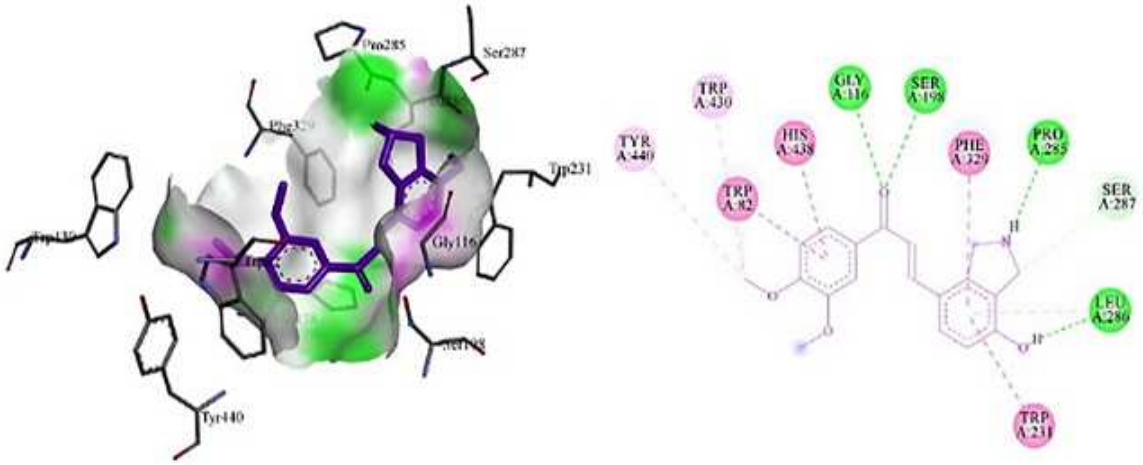

Fig. 9: 3D, 2D interaction of BuChE with novel compound (utilito)

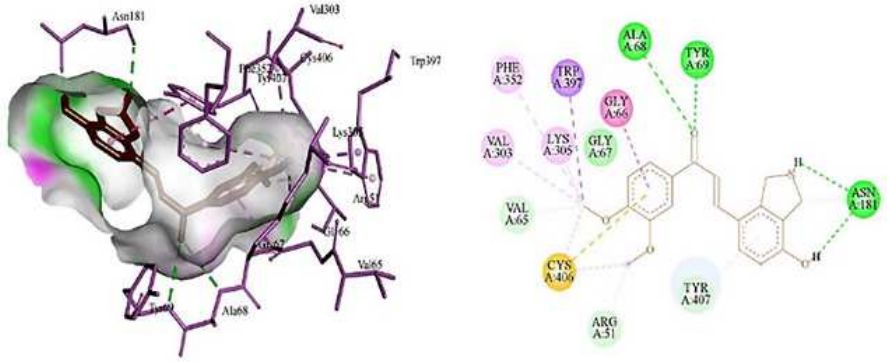

Fig. 10: 3D, 2D interaction of MAO-A with novel compound (utilito)

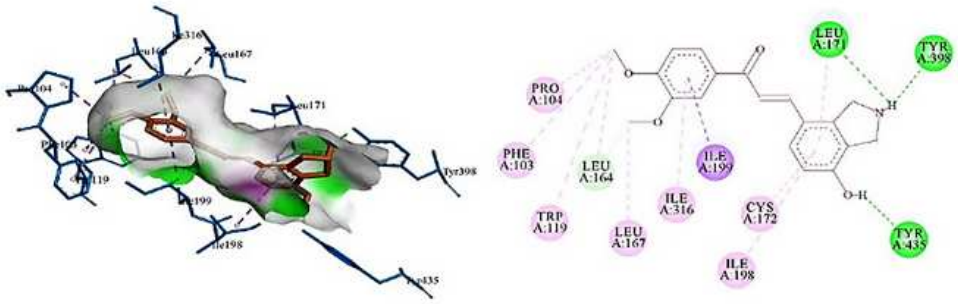

Fig. 11: 3D, 2D interaction of MAO-B with novel compound (utilito)

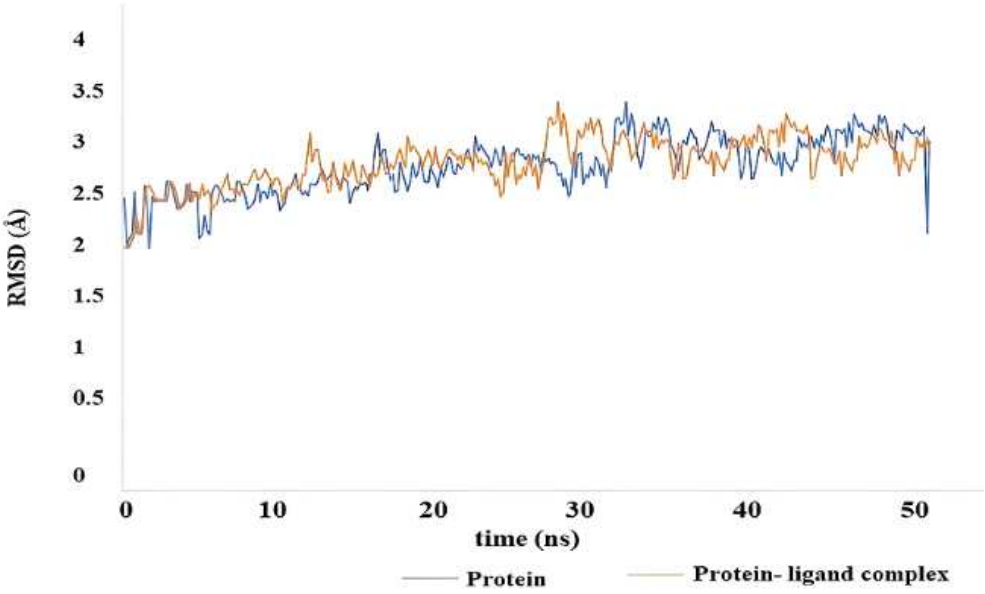

Fig. 12: Root mean square deviation (RMSD) of AChE and utilito complex as function of time

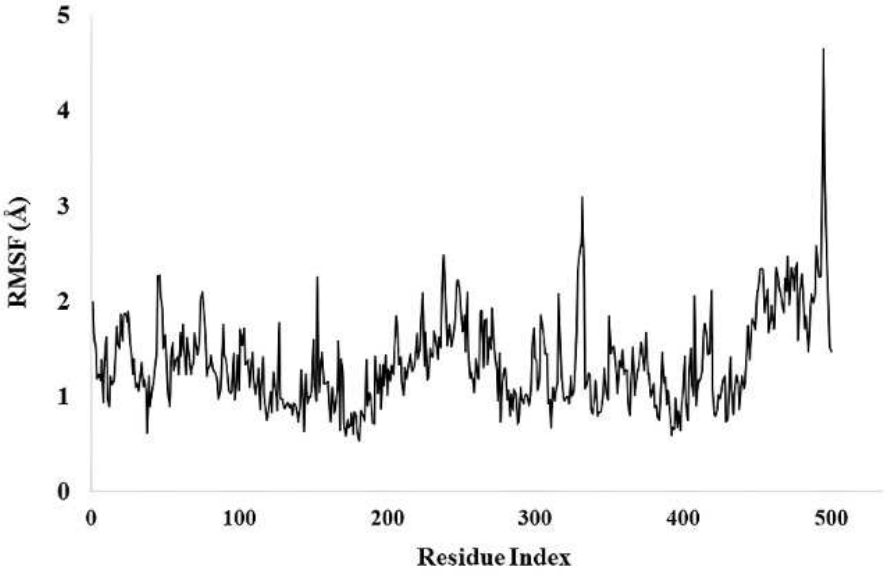

Fig. 13: Root mean square fluctuation (RMSF) of Cα atoms of complex AChE- novel compound (utilito)

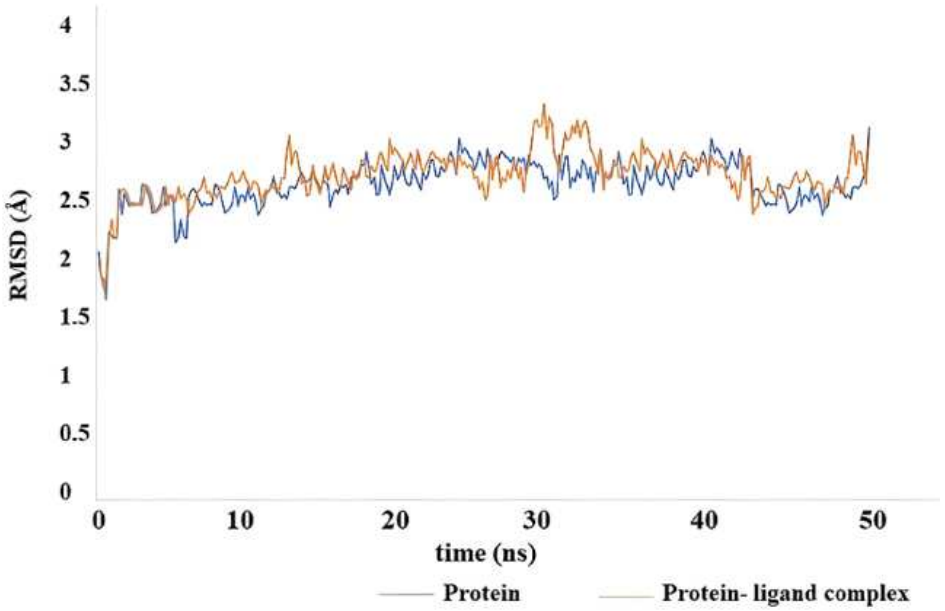

Fig. 14: Root mean square deviation (RMSD) of MAO-B, MAO-B and utilito complex as function of time

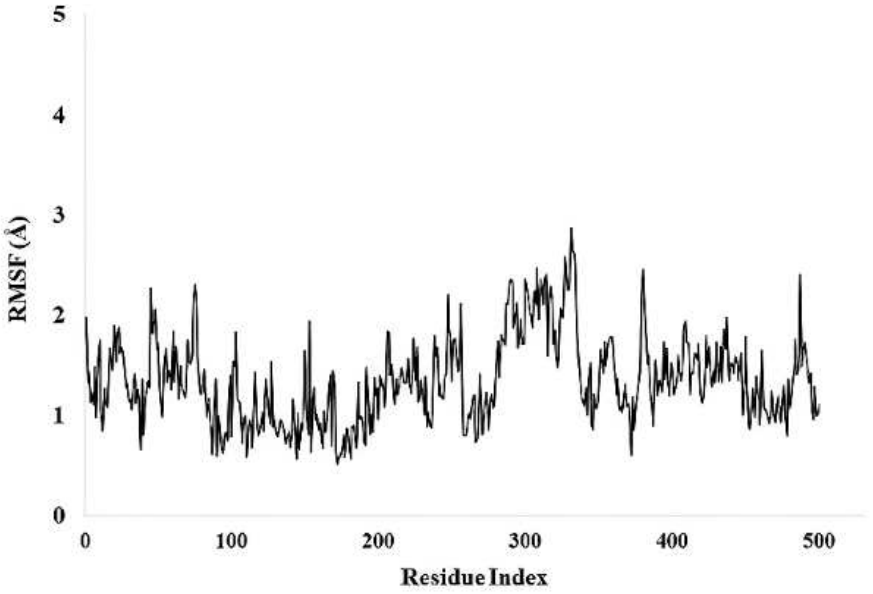

Fig. 15: Root mean square fluctuation (RMSF) of Cα atoms of complex MAO-B- utilito

We applied molecular docking studies to understand the binding interaction between the chalcone derivative (Utilito) and MAO-B and showed strong binding affinity of utilito with MAO-B) with docking scores of - 41.4 kJ/mol compared to acetylcholinesterase (AChE) -41.2 kJ/mol as shown in table 10. Conventional hydrogen bond interactions between MAO-B residue LEU171, TYR398, TYR435, and the phenol ring of utilito were observed. This theoretical prediction was confirmed by later in vivo biochemical tests, which offered solid proof of utilito's anti-oxidative activity.

The structural feature of the planarity and hydrophobicity of the chalcone derivative (Utilito) led it to bind directly, thus inhibiting the degradation of dopamine into neurotoxic metabolites, in the active site of the enzyme(Ipe *et al*., 2024). Moreover, the chalcone (Utilito) derivative decreased the generation of hydrogen peroxide (H2O2) in the process of deamination, which is important in limiting the formation of hydroxyl radicals, another potent source of oxidative stress in the brain. All these findings help to corroborate the greater clinical usefulness of this compound not only for Alzheimer's but also for

other neurodegenerative diseases where oxidative stress plays a major role. Moreover, further studies should be conducted in animal models and clinical trials to ascertain its therapeutic efficacy and optimize its use as part of a broader treatment regimen for neurodegenerative disorders (Krishna *et al*., 2023).. Because the chalcone derivative (Utilito) inhibited MAO-B and subsequently reduced ROS production, it might exert a dual benefit: it would protect neurons from oxidative damage as well as relieve cellular stress that underlies the pathophysiology of Alzheimer's disease (Riederer *et al*., 2004). Utilito produced marked enhancements in memory and cognitive performance in treated rats. In the Y-maze, a clear dose-dependent increase in spontaneous alternation was observed, reaching 37.35% at 300 mg/kg, a level comparable to that achieved with rivastigmine (37.33%), whereas the disease control group showed no alternation. Similarly, in the Morris water maze, Utilito-treated animals demonstrated significantly shorter escape latencies, indicating improved spatial learning and memory. The open-field test further revealed substantial increases in locomotion and exploratory behaviour, signifying restored cognitive and motor function typically compromised in Alzheimer's disease models (Asadzadeh Bayqara *et al*., 2024b). Biochemical analyses corroborated these behavioral improvements. Utilito administration elevated endogenous antioxidant enzyme levels, specifically superoxide dismutase (SOD) and catalase (CAT), while significantly reducing malondialdehyde (MDA) by approximately 40%. These results suggest that Utilito bolsters neuronal defenses against oxidative damage associated with AD (Dhapola *et al*., 2024b; Agostinho *et al*., 2010). Utilito also contains anti-oxidant activity (71 ± 0.11%) in the DPPH assay. Further, the chalcone derivative (Utilito) causes a remarkable increase in SOD and CAT activities, which are well-known enzymatic scavengers for ROS. This enhanced activity of antioxidant enzymes indicates that the chalcone derivative (Utilito) is not only directly scavenging ROS but also enhancing the endogenous antioxidant defense of the brain. Such a reduction in oxidative stress may also have important implications for the function of mitochondria. (Tönnies and Trushina, 2017). Oxidative stress damages mitochondria, and this is what accounts for impaired ATP production, mitochondrial dysfunction, and neuronal apoptosis in Alzheimer's disease. An ability of the chalcone derivative to reduce oxidative stress might help preserve mitochondrial function and support neuronal survival, and thus cognitive function. It addresses one of the most crucial aspects of Alzheimer's disease pathophysiology by protecting mitochondria and improving energy metabolism (Firdous *et al*., 2024, Behl *et al*., 2021).

In addition to oxidative stress, neuroinflammation has emerged as critical and pivotal in the pathogenesis of AD). Recent studies have highlighted that neuroinflammation is not only a consequence of neuronal injury but rather a central mechanism driving the progression of the disease (Heneka *et al*., 2015). One of the first responses to the formation of tau tangles, amyloid-beta plaques and other hallmarks of pathological neurodegeneration in AD, such as astrocytes and microglia activation, and the brain's resident immune cells. These immune cells become activated upon the accumulation of these toxic protein aggregates and release various pro-inflammatory cytokines and chemokines (Calsolaro and Edison, 2016, Domingues *et al*., 2017). In AD, chronic activation of glial cells-particularly microglia and astrocytes-plays a central role in sustaining neuroinflammation. Normally, microglia help maintain brain homeostasis by clearing debris and supporting neurons, but in a diseased state, they release pro-inflammatory mediators that worsen neuronal damage. Similarly, reactive astrocytes produce cytokines and other inflammatory substances that contribute to neurodegeneration. This persistent inflammatory response creates a vicious cycle that amplifies neuronal dysfunction and accelerates disease progression (Heneka and O'Banion, 2007). In Alzheimer's disease, reactive astrocytes produce pro-inflammatory substances, which further damage the adjacent neurons. The chronic inflammatory environment resulting from these cellular responses characterizes AD and promotes the progression of decline in cognitive functions and memory (Avila-Muñoz and Arias, 2014).

Our results indicate that the chalcone derivative (Utilito) isolated from *Arisaema utile* is endowed with considerable neuroprotection, especially against the outcomes of neuroinflammation (Bhat *et al*., 2019). Although we did not measure the levels of cytokines in this study, the marked reduction of oxidative stress and neurodegeneration among the treated animals suggests that it might act by inhibiting microglia and astrocyte activation. The mentioned above cells have a significant function in the neuroinflammatory reaction that is associated with AD. Activation of these cells usually leads to the synthesis of inflammatory mediators, including interleukin-6 (IL-6) interleukin-1 beta (IL-1β), and tumor necrosis factor-alpha (TNF-α) (Kany *et al*., 2019). The cytokines are then released, causing further neuronal damage and synaptic dysfunction. Thus, by inhibiting oxidative stress and the microglia and astrocytes activation process, this chalcone derivative (Utilito) may successfully decrease the levels of all these pro-inflammatory cytokines, which would then reduce the overall neuroinflammatory burden. (Castellani *et al*., 2010, Dhapola *et al*., 2024)

Our study's findings suggest that the chalcone derivative (Utilito) was a more well-rounded therapeutic strategy that could treat these fundamental aspects of the disease. It may not just improve cognitive performance, but the chalcone derivative (Utilito) is of great potential as a

multitarget therapeutic agent for AD (Bhat *et al*., 2019). This compound has the potential to inhibit MAO-B, reduce oxidative stress, and attenuate neuroinflammation, indicating that it has a significant role in the cure of AD than the traditional monotherapy approach, where in one pathological aspect of the disease is targeted (Siddiqui *et al*., 2023, Jose *et al*., 2024). Another significant challenge to treating the AD efficiently is the permeability of the BBB by therapeutic compounds. The selective barrier, such as the BBB that limits the entry of most drugs into the central nervous system (CNS). Given that the chalcone derivative (utilito) is relatively lipophilic, it is likely to exhibit good bioavailability in the brain, which is a critical factor for the effectiveness of any central nervous system-targeting drug (Bors and Erdő, 2019; Ipe *et al*., 2024).

However, several limitations remain. First, the lack of cytokine profiling prevents full investigation of potential anti-inflammatory actions. Second, the study did not include pharmacokinetic analyses such as ADME profiling or assessments of blood–brain barrier (BBB) penetration, which are crucial for CNS-active agents. Third, there is insufficient data on long-term toxicity and chronic dosing, leaving questions regarding Utilito's safety unresolved. Follow-up studies should address these critical areas to determine their therapeutic viability for AD. All results are statistically analysed, and the number of animals in each group is six to statistically justify the findings.

In the future much more research is needed to fully understand the mechanisms of action of the chalcone derivative (Utilito) as well as to evaluate pharmacokinetics, particularly its ADME profiles, long-term safety, and efficacy in preclinical and clinical settings. This study highlights the importance of chalcone derivatives (Utilito) as a new class of compounds to be further explored for potential applications in the treatment of AD and other neurodegenerative disorders, in the hope of a better, integrative, and durable therapy.

CONCLUSION

The phytochemical investigation on the plant, i.e. *Arisaema utile,* resulted in the isolation and identification of novel compounds, such as chalcone derivative (Utilito) has been found to be a potent neuroprotective agent in experimental models so it is suggesting the potential of chalcone derivative (Utilito) as a therapeutic agent for the treatment of AD. The isolated compound also has potent antioxidant activity to treat cellular damage as well as oxidative stress-related ailments. The biochemical evaluation highlighted that chalcone also has good antioxidant activity. Moreover over the chalcone derivatives (Utilito) rich extract showed enhanced cognitive effect in AD.

Conflict of interest

The authors declare no conflict of interest.

REFERENCES

Agostinho P, R A Cunha and C Oliveira (2010). Neuroinflammation, oxidative stress and the pathogenesis of Alzheimer's disease. *Curr. Pharm. Des.* **16**(25): 2766-2778.

Akhter N, I Rafiq, A Jamil, Z Chauhdary, A Mustafa, AJB Nisar and BR Communications (2025). Neuroprotective effect of Thymus vulgaris on paraquat induced Parkinson's disease. *Biochem Biophys Res Commun.* **761**: 151740.

Asadzadeh Bayqara S, M Aghazadeh Yamchelu, S Abdolahzadeyadegari, M Farhadi, S Nadjafi, J Fahanik Babaei and N Hosseini (2024). The effects of a chalcone derivative on memory, hippocampal corticosterone and BDNF levels in adult rats. *Int. J. Neurosci.,* **134**(3): 214-223.

Avila-Muñoz E and C Arias (2014). When astrocytes become harmful: Functional and inflammatory responses that contribute to Alzheimer's disease. *Ageing Res. Rev.,* **18**: 29-40.

Barclay PL and DZ Zhang (2021). Periodic boundary conditions for arbitrary deformations in molecular dynamics simulations. *J. Comput. Phys.* **435**: 110238.

Behl T, D Kaur, A Sehgal, S Singh, N Sharma, G Zengin, FL Andronie-Cioara, MM Toma, S Bungau and AG Bumbu (2021). Role of monoamine oxidase activity in Alzheimer's disease: An insight into the therapeutic potential of inhibitors. *Molecules.* **26**(12): 3724.

Bhat AH, A Alia, GM Rather and B Kumar (2019). Isolation & characterisation of beta-sitosterol from the rhizomes of Arisaema utile and its evaluation for antioxidant activity. *Int. J. Sci. Res. Biol. Sci. Vol.,* **6**: 111-118.

Bibi Y, S Nisa, FM Chaudhary and M Zia (2011). Antibacterial activity of some selected medicinal plants of Pakistan. *BMC Complement Altern Med.,* **11**(1): 52.

Binda C, J Wang, L Pisani, C Caccia, A Carotti, P Salvati, DE Edmondson and A Mattevi (2007). Structures of human monoamine oxidase B complexes with selective noncovalent inhibitors: Safinamide and coumarin analogs. *J. Med. Chem.,* **50**(23): 5848-52.

Bors LA and F Erdo (2019). Overcoming the blood–brain barrier. challenges and tricks for CNS drug delivery. *Sci. Pharm.* **87**(1): 6.

Bowers KJ, E Chow, H Xu, RO Dror, MP Eastwood, BA Gregersen, JL Klepeis, I Kolossvary, MA Moraes and FD Sacerdoti. Scalable algorithms for molecular dynamics simulations on commodity clusters. Proceedings of the 2006 ACM/IEEE Conference on Supercomputing, 2006. 84-es.

Calsolaro V and P Edison (2016). Neuroinflammation in Alzheimer's disease: Current evidence and future directions. *AD/ADRD.* **12**(6): 719-732.

Castellani RJ, RK Rolston and MA Smith (2010). Alzheimer Disease. *Disease-a-Month.* **56**(9). 484-546.

Chen Y-F, S-N Wu, J-M Gao, Z-Y Liao, Y-T Tseng, F Fulop, F-R Chang and Y-C Lo (2020). The antioxidant, anti-inflammatory, and neuroprotective properties of the synthetic chalcone derivative AN07. *Molecules.* **25**(12): 2907.

De Colibus L, M Li, C Binda, A Lustig, DE Edmondson and A Mattevi (2005). Three-dimensional structure of human monoamine oxidase A (MAO A): Relation to the structures of rat MAO A and human MAO B. *ProcNatl Acad Sci USA.,* **102**(36): 12684-12689.

Dhapola R, SK Beura, P Sharma, SK Singh and D Harikrishnareddy (2024). Oxidative stress in Alzheimer's disease: Current knowledge of signaling pathways and therapeutics. *Mol. Biol. Rep.* **51**(1): 48.

Domingues C, O Ab Da Cruz E Silva and A Henriques (2017). Impact of cytokines and chemokines on Alzheimer's disease neuropathological hallmarks. *Curr. Alzheimer Res.,* **14**(8): 870-882.

Du SS, HM Zhang, CQ Bai, CF Wang, QZ Liu, ZL Liu, YY Wang and ZW Deng (2011). Nematocidal flavone-C-glycosides against the root-knot nematode (Meloidogyne incognita) from Arisaema erubescens tubers. *Molecules.* **16**(6): 5079-86.

Ekundayo TC, TA Olasehinde, K Okaiyeto and AI Okoh (2021). Microbial Pathogenesis and Pathophysiology of Alzheimer's Disease: A Systematic Assessment of Microorganisms' Implications in the Neurodegenerative Disease. *Front. Neurosci.,* **15**: 648484.

Finberg JP and JM Rabey (2016). Inhibitors of MAO-A and MAO-B in psychiatry and neurology. *Front. Pharmacol.,* **7**: 209773.

Firdous SM, SA Khan and A Maity (2024). Oxidative stress–mediated neuroinflammation in Alzheimer's disease. *N-S Arch Pharmacol.*, pp.1-21.

Gao H-M, H Zhou and J-S Hong (2014). Oxidative stress, neuroinflammation and neurodegeneration. *In:* Phillip K. Peterson MT Neuroinflammation and neurodegeneration. 1st ed., Springer New York, pp.81-104.

Gaur K and YH Siddique (2024). Effect of apigenin on neurodegenerative diseases. *Neurol. Disord. Drug Targets.* **23**(4): 468-475.

Goldstein DB (1968). A method for assay of catalase with the oxygen cathode. *Anal. Biochem.,* **24**(3): 431-437.

Guckel EK (1999). Large scale simulations of particulate systems using the PME method, University of Illinois at Urbana-Champaign.

Heneka MT, MJ Carson, J El Khoury, GE Landreth, F Brosseron, DL Feinstein, AH Jacobs, T Wyss-Coray, J Vitorica and RM Ransohoff (2015). Neuroinflammation in Alzheimer's disease. *Lancet Neurol.,* **14**(4): 388-405.

Ipe R, JM Oh, S Kumar, I Ahmad, LR Nath, S Bindra, H Patel, KY Kolachi, P Prabhakaran and P Gahtori (2024). Inhibition of monoamine oxidases and neuroprotective effects: Chalcones vs. chromones. *Molecular Diversity.* 1-17.

Jose J, JK Varughese, MK Parvez and TV Mathew (2024). Probing the inhibition of MAO-B by chalcones: An integrated approach combining molecular docking, ADME analysis, MD simulation, and MM-PBSA calculations. *J. Mol. Model.* **30**(4). 103.

Kakkar R, J Kalra, SV Mantha, KJM Prasad and C Biochemistry (1995). Lipid peroxidation and activity of antioxidant enzymes in diabetic rats. *Mol Cell Biochem.* **151**:113-119.

Kany S, JT Vollrath and B Relja (2019). Cytokines in inflammatory disease. *Int. J. Mol. Sci.,* **20**(23): 6008.

Kim S, J Lee, S Jo, CL Brooks Iii, HS Lee and W Im 2017. CHARMM-GUI ligand reader and modeler for CHARMM force field generation of small molecules. Wiley Online Library.

Krishna A, S Kumar, ST Sudevan, AK Singh, LK Pappachen, T Rangarajan, MA Abdelgawad and B Mathew (2024). A comprehensive review of the docking studies of chalcone for the development of selective MAO-B inhibitors. *CNS Neurol. Disord.,* **23**(6): 697-714.

Krishna A, J Lee, S Kumar, ST Sudevan, P Uniyal, LK Pappachen, H Kim and B Mathew (2023). Inhibition of monoamine oxidases by benzimidazole chalcone derivatives. *Appl Biol Chem.,* **66**(1): 37.

Lakshmi B, M Sudhakar and KSJBTER Prakash (2015). Protective effect of selenium against aluminum chloride-induced Alzheimer's disease: Behavioral and biochemical alterations in rats. *Biol Trace Elem Res.,* **165**(1): 67-74.

Lam K, K Pan, JF Linnekamp, JP Medema and RJBEBa-ROC Kandimalla (2016). DNA methylation based biomarkers in colorectal cancer: A systematic review. **1866**(1): 106-120.

Li X, X Feng, X Sun, N Hou, F Han and Y Liu (2022). Global, regional, and national burden of Alzheimer's disease and other dementias, 1990-2019. *Front Aging Neurosci.* **14**: 937486.

Li X, Y Li, Z Liu, Q Zhang, Y Zhou, L Yu, W Liu and Z Sang (2024). Development of novel chalcone derivatives as multifunctional agents for the treatment of Alzheimer's disease. *Med Chem Res.,* **3**(1): 548 - 561.

Lim B, I Prassas and EP Diamandis (2021). Alzheimer disease pathogenesis: The role of autoimmunity. *J. Appl. Lab. Med.* **6**(3): 756-764.

Lin P, J Sun, Q Cheng, Y Yang, D Cordato and J Gao (2021). The Development of Pharmacological Therapies for Alzheimer's Disease. *Neuro and Therapy.* **10**(2): 609-626.

Marchon ISDS, EDDN Melo, MDC Botinhão, GN Pires, JVR Reis, ROMA De Souza, ICR Leal, AGC Bonavita, HR Mendonça and MF Muzitano (2024).

Pharmacological potential of 4-dimethylamino chalcone against acute and neuropathic pain in mice. *J. Pharm. Pharmacol.* rgae057.

Morris GM, R Huey, W Lindstrom, MF Sanner, RK Belew, DS Goodsell and AJ Olson (2009). AutoDock4 and AutoDockTools4: Automated docking with selective receptor flexibility. *J. Comput. Chem.,* **30**(16): 2785-2791.

Nachon F, E Carletti, C Ronco, M Trovaslet, Y Nicolet, L Jean and PY Renard (2013). Crystal structures of human cholinesterases in complex with huprine W and tacrine: elements of specificity for anti-Alzheimer's drugs targeting acetyl- and butyryl-cholinesterase. *Biochem J.,* **453**(3): 393-9.

Nguyen VB, S-L Wang, AD Nguyen, Z-H Lin, CT Doan, TN Tran, HT Huang and Y-H Kuo (2018). Bioactivity-guided purification of novel herbal antioxidant and anti-NO compounds from Euonymus laxiflorus Champ. *Molecules.* **24**(1): 120.

Ramsay RR and A Albreht (2018). Kinetics, mechanism, and inhibition of monoamine oxidase. *J. Neural Transm.* **125**(11): 1659-1683.

Ravi SK, BN Ramesh, R Mundugaru, BJET Vincent and Pharmacology (2018). Multiple pharmacological activities of Caesalpinia crista against aluminium-induced neurodegeneration in rats: Relevance for Alzheimer's disease. *Environ Toxicol Pharmacol.* **58**: 202-211.

Riederer P, W Danielczyk and E Grünblatt (2004). Monoamine oxidase-B inhibition in Alzheimer's disease. *Neurotoxicology.* **25**(1-2): 271-277.

Rojas RJ, DE Edmondson, T Almos, R Scott and ME Massari (2015). Reversible and irreversible small molecule inhibitors of monoamine oxidase B (MAO-B) investigated by biophysical techniques. *Bioorg. Med. Chem.,* **23**(4): 770-778.

Saadullah M, H Tariq, Z Chauhdary, U Saleem, S Anwer Bukhari, A Sehar, M Asif and A Sethi (2024). Biochemical properties and biological potential of Syzygium heyneanum with antiparkinson's activity in paraquat induced rodent model. *Plos One.,* **19**(3): e0298986.

Saleem U, Z Raza, F Anwar, B Ahmad, S Hira and TJM Ali (2019). Experimental and computational studies to characterize and evaluate the therapeutic effect of Albizia lebbeck (L.) seeds in Alzheimer's disease. *Evid Based Complement Alternat Med.,* **55**(5): 184.

Savithramma N, ML Rao and D Suhrulatha (2011). Screening of medicinal plants for secondary metabolites. *J. Sci. Res.,* **8**(3): 579-584.

Siddiqui AJ, S Jahan, MA Siddiqui, A Khan, MM Alshahrani, R Badraoui and M Adnan (2023). Targeting monoamine oxidase B for the treatment of Alzheimer's and Parkinson's diseases using novel inhibitors identified using an integrated approach of machine learning and computer-aided drug design. *Mathematics.* **11**(6): 1464.

Siddiqui N, M Talib, PN Tripathi, A Kumar and A Sharma (2024). An insight into the neurodegenerative exploration of Baicalein: A review. *Health Sci. Rev.,* 100172.

Singla RK, K Dhonchak, RK Sodhi, M Arockia Babu, J Madan, R Madaan, S Kumar, R Sharma and BJFIP Shen (2022). Bergenin ameliorates cognitive deficits and neuropathological alterations in sodium azide-induced experimental dementia. **13**: 994018.

Son SY, J Ma, Y Kondou, M Yoshimura, E Yamashita and T Tsukihara (2008). Structure of human monoamine oxidase A at 2.2-A resolution: the control of opening the entry for substrates/inhibitors. *Proc Natl Acad Sci U S A.* **105**(15): 5739-44.

Tabassum S, M Zia, EJ Carcahe De Blanco, R Batool, R Aslam, S Hussain, Q Wali and MM Gulzar (2019). Phytochemical, in-vitro biological and chemo-preventive profiling of Arisaema jacquemontii Blume tuber extracts. *BMC Complement. Altern. Med.,* **19**(1): 256.

Tarragon E, D Lopez, C Estrada, GC Ana, E Schenker, F Pifferi, R Bordet, JC Richardson, MTJCN Herrero and Therapeutics (2013). Octodon degus: A model for the cognitive impairment associated with a lzheimer's disease. **19**(9): 643-648.

Tönnies E and E Trushina (2017). Oxidative stress, synaptic dysfunction, and Alzheimer's disease. *J Alzheimer Dis.,* **57**(4): 1105-1121.

Wang X, W Wang, L Li, G Perry, H-G Lee and X Zhu (2014). Oxidative stress and mitochondrial dysfunction in Alzheimer's disease. *BBA - Mol. Basis Dis.,* **1842**(8): 1240-1247.

Zhang R-Y, X Zhang, L Zhang, Y-C Wu, X-J Sun and LJCHM Li (2021). Tetrahydroxystilbene glucoside protects against sodium azide-induced mitochondrial dysfunction in human neuroblastoma cells. **13**(2): 255-260.